A Numerical Study of 3D Kelvin Cell Arrangements as a Basis for Locally Resonant Acoustic Metamaterials

Lukas Kleine-Wächter[1], Huina Mao[2,3], Romain Rumpler[2,3], Matthias Miksch[1], Quirin Aumann[1], Gerhard Müller[1]

[1] *Chair of Structural Mechanics, Technical University of Munich, 80333 Munich, Germany*

[2] *MWL Laboratory for Sound and Vibration Research, KTH Royal Institute of Technology, SE-100 44 Stockholm, Sweden*

[3] *The Centre for ECO2 Vehicle Design, KTH Royal Institute of Technology, SE-100 44 Stockholm, Sweden*

Email: lukas.kleinewaechter@tum.de

Introduction

Locally resonant acoustic metamaterials (LRAM) have been attracting increasing attention in the past two decades due to their ability to influence wave propagation in targeted frequency bands. In these bands, significant vibration attenuation is achievable from the interaction between a host structure and structural subunits designed to resonate out-of-phase with respect to the motion of the host structure. The dimensions of resonant units may be smaller than the wavelength of the affected waves, thus allowing compact and lightweight designs with enhanced vibroacoustic properties while maintaining a high stiffness-to-mass ratio of the overall structure [1]. For that reason, LRAMs are particularly interesting for industrial applications. Yet, due to the narrow-banded nature of resonances, metamaterial-based approaches for broadband vibration attenuation performances, especially in the lower-frequent regime, remain a challenge [2].

Accompanied by the development of additive manufacturing, three-dimensional cellular structures have emerged as a novel concept to develop LRAMs for broadband attenuation performance. Such architectures are often composed of cellular lattices that are typically periodically repeated in space to form the microstructure. Lattices are multi-degree-of-freedom structures providing multiple vibration modes that can be exploited to affect vibrations in different frequency regimes and thus broaden the bands of vibration attenuation. As a result, a cellular structure can function as a multi-resonator in itself without the need for embedded resonant units. Recent numerical and experimental investigations have shown that broadband vibration attenuation is achievable by employing cellular architectures for locally resonant metamaterials [2–4].

The dynamic properties of a unit cell lattice are strongly affected by its topology and, therefore, may be dynamically tuned by adjusting the characteristic parameters of the lattice. Furthermore, through modifying individual parts of the lattice, spatially varying stiffness and density are achievable, linked with the anisotropy of the corresponding macroscopic properties [5].

This contribution discusses the potential of cellular metaresonators for low-frequency vibration attenuation based on Kelvin cell (KC) arrangements. The Kelvin cell design is modified by imposing geometrical transformations to the reference design, aiming to provide an additional tuning mechanism of the dynamic properties of the structure. After outlining the unit cell design and the devised tuning approach, the KC and a selection of modified unit cells are investigated concerning their vibrational characteristics to demonstrate the effects of geometrical transformations. A vibroacoustic test scenario is employed, and assemblies of two cells are added to the core of a sandwich structure to improve the sound transmission behavior and test the applicability of the proposed design approach. The research presented builds upon initial contributions by some of the co-authors [6–8].

Kelvin Cell & Transformation Approach

The Kelvin cell (KC) is deduced from a tetrakaidecahedron, see Fig. 1. The unit cell features 6 square and 8 hexagonal faces formed by a network of 36 ligaments. Each of the 24 vertices rigidly connects the ends of coinciding ligaments. The cell exhibits isometry with a characteristic length h_c and cubic material symmetry. The KC architecture is assumed to provide a manufacturable multi-functional lattice structure that is lightweight and sufficiently stiff for load-bearing purposes, with diverse vibration modes being exploitable for vibration attenuation performances. In this context, lattice adaptations such as functional grading and inertia amplification by embedded masses are further prospects.

The KC structure enables geometric modifications in a relatively straightforward manner. In the following, the idea of *twisting* the KC structure is considered, as a key factor to investigate an additional tuning mechanism of underlying cell dynamics.

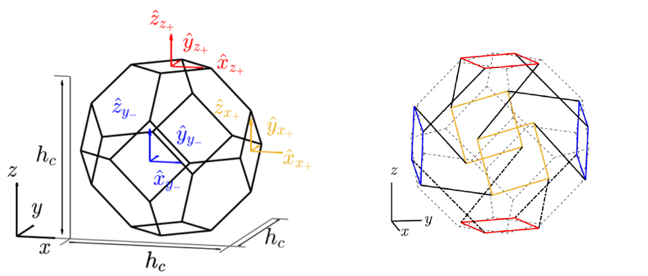

Figure 1: Isometric KC reference and coordinate definitions (left) and geometry after twisting all six square faces (right) [6].

Geometrical modifications imposed to the reference geometry are achieved through coordinate transformations that describe pairwise rigid body rotations of the cell's square faces. The rotational angles applied to opposing square faces are anti-symmetric, thus of opposite sign, and equal in absolute value. Thereby, twisted cells exhibit chirality with respect to each middle plane parallel to the pairs of twisted faces. It is further presumed that the squares are undeformed after rotation, and all vertices remain connected through the same ligaments with altered lengths compared to the isometric reference geometry. Thus, the modified structure still forms a well-defined unit cell and is topologically equivalent to the isometric structure. Various ways to apply rotations exist as demonstrated by Mao et al. [7], however, this study solely focuses on *twisting* the KC, meaning in-plane rotations of the square faces with respect to their local coordinates. The sets of local coordinates $(\hat{x}, \hat{y}, \hat{z})_j$ originate at the center of the respective square faces denoted j and are parallel to the isometric cell's global coordinates (x, y, z) as shown in Fig. 1. Transformations between the local and global coordinate systems are expressed using Euler rotation angles $[\theta_j^{\hat{x}}, \theta_j^{\hat{y}}, \theta_j^{\hat{z}}]$. Assuming successive, independent rotations around the axes $\hat{z}$, $\hat{y}$ and $\hat{x}$, the rotation matrices read

$$[R]_j = \begin{bmatrix} 1 & 0 & 0 \\ 0 & c.\theta_j^{\hat{x}} & -s.\theta_j^{\hat{x}} \\ 0 & s.\theta_j^{\hat{x}} & c.\theta_j^{\hat{x}} \end{bmatrix} \begin{bmatrix} c.\theta_j^{\hat{y}} & 0 & s.\theta_j^{\hat{y}} \\ 0 & 1 & 0 \\ -s.\theta_j^{\hat{y}} & 0 & c.\theta_j^{\hat{y}} \end{bmatrix} \begin{bmatrix} c.\theta_j^{\hat{z}} & -s.\theta_j^{\hat{z}} & 0 \\ s.\theta_j^{\hat{z}} & c.\theta_j^{\hat{z}} & 0 \\ 0 & 1 & 0 \end{bmatrix} \quad (1)$$

with $c.\cdot = \cos(\cdot)$ and $s.\cdot = \sin(\cdot)$. Consequently, the location of points $(\hat{x}, \hat{y}, \hat{z})_j^T$ at the square face j of the KC reference lattice is given by

$$(\hat{x}', \hat{y}', \hat{z}')_j^T = [R]_j \, (\hat{x}, \hat{y}, \hat{z})_j^T \quad (2)$$

after twisting the isometric structure. The concept of twisting is expected to add another variable to the unit cell design, allowing for the parametric design of cell architectures with substantially differing dynamic properties but with identical material and lattice settings and the same topology.

Eigenfrequency Analysis

To investigate the tunability of the dynamic properties of the twisted KCs, an eigenfrequency analysis is carried out using finite element models obtained from COMSOL Multiphysics. Two different setups are considered: First, one-axial twists of a single pair of opposing faces and twist angles between 0° and 90°; second, two- and three-axial ('full') twists at a constant angle of 90°. Examples of tested structures are depicted in Fig. 2. It is noted that potential side effects of twisting such as a locally increased stiffness due to an increasing ligament overlap at the connection points are neglected. Geometry and the material parameters are summarized in Tab. 1. Circular cross-sections are assumed for the ligaments. The material parameters represent a polymeric material used

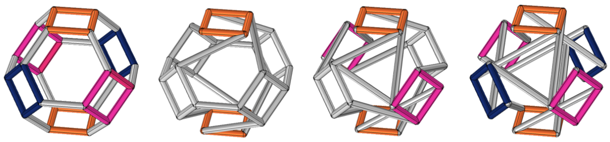

Figure 2: Isometric Kelvin cell (left) and examples of one, two-, and three-axial twists with $\theta_j = 90°$ (left to right). Colors indicate rotated square faces.

in additive manufacturing. All structures are meshed with tetrahedral quadratic elements; a convergence check allowed to ensure a proper discretization. The eigenfrequencies of a selection of tested arrangements are depicted in Fig. 3 with respect to the modal order. With an increasing twist angle, there is a clear trend of shifting eigenfrequencies towards lower frequencies compared to the isometric cell. This effect bears upon the deformation mechanism of modes that are dominated by the individual bending deformation of ligaments. Given the premises of twisting, ligaments connected to twisted faces are elongated as compared to the isometric KC which may be associated with lower eigenvalues of corresponding modes and overall softening behavior of twisted cells. The tuning effect manifests even more distinctly for the 90° two-axial and fully-twisted cells with a drop of almost 1 kHz between the first mode of the fully twisted and isometric structure. Furthermore, twisting influences the spacing of eigenfrequencies. The isometric cell exhibits a staircase-shaped progression of modes that is traceable to its cubic-symmetry evoking multiple eigenvalues corresponding to multi-axial bending. Twisting the cell breaks the symmetry and establishes chirality between rotated opposing square faces. Associated multiple eigenvalues are, therefore, reduced resulting in an increased modal density as can be particularly seen at the 60° twist. Vice versa, the full-axial twisting replicates ligaments of equal lengths which is linked with an increased multiplicity of eigenvalues as can be seen at 835 Hz. From these initial considerations, it stands to reason that twisting may provide a way to modulate the resonances of an emerging cellular material and the formation of bandgaps.

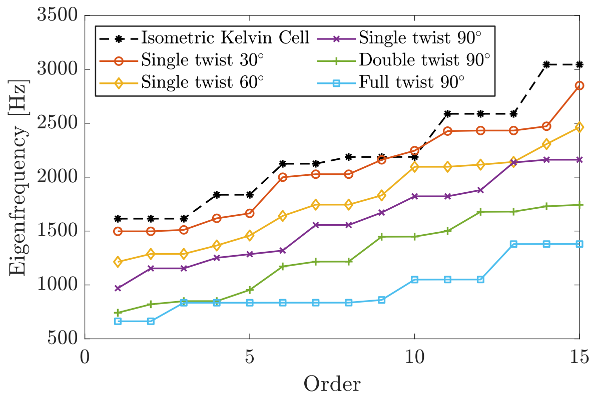

Figure 3: First 15 eigenfrequencies of the isometric Kelvin cell and twisted structures. For all geometries, a characteristic length $h_c = 25$ mm and circular ligament cross-sections with a diameter of $d = 1.5$ mm were chosen.

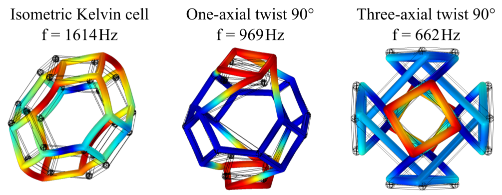

Figure 4: Deformations of the first mode shape of the isometric, one- and three-axial twisted cell. Twisted structures exhibit extension-torsion coupling effects.

Apart from tuning effects, introducing twists influences the deformation behavior of selected mode shapes and enforces extensional-torsion coupling effects. As an illustration, Fig. 4 compares the first mode of the isometric, one-axial and three-axial twisted cells. Chiral-symmetric square faces exhibit local reverse rotation movements linked with the bending movement of connecting ligaments. Observations on further structures not discussed within this contribution indicate that such coupling is more likely to occur with increasing twist angles. When twisting three-axially, an overall extensional-torsional coupled deformation is observable, indicating that extension-compression deformation of the cell will cause torsional deformation around its square faces. As a result, twisting may provide a way to tailor a coupled translational-rotational resonator with square faces serving as a host for mass inclusions that might amplify the rotational inertial properties. Ongoing work considers the representation of the effects of the twisting in terms of the dispersion characteristics of the resonator and its extension-torsion coupling properties.

Vibroacoustic Application

A metamaterial application case following contributions of Liu et al. [9] is presented to validate the applicability of the KC concept for sound insulation purposes. Arrays assembled from two KCs are employed in a sandwich panel to generate a resonator-like behavior. Fig. 5 presents the considered numerical model; Tab. 1 shows the linear-elastic material properties. The FE model was implemented in COMSOL Multiphysics. Displacements and velocities of the solid parts of the sandwich panel are computed with the sandwich regarded as an isotropic elastic material. The incident and transmitted fields are simulated using the 'background pressure field' option. Infinite and non-reflecting sound fields are implemented by setting plane wave radiation conditions at the upper and lower boundaries of the acoustic domain. In the example, plane waves impinge on the structure with an

Table 1: Material parameters of the KC and sandwich panel as shown in Fig. 5. η denotes the loss factor.

Material	E [GPa]	ρ [kg/m^3]	ν [1]	η [1]
Kelvin Cell	1.3	1100	0.30	-
Core	0.8	920	0.30	0.010
Aluminum	69	2700	0.33	0.001

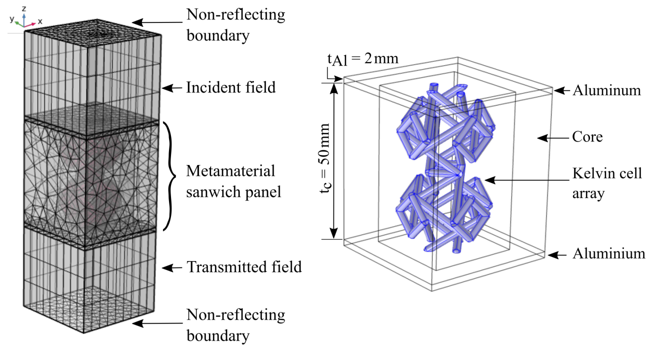

Figure 5: Numerical Model according to Liu et al. [9].

angle of 60° with respect to the vertical z-axis as shown in Fig. 5. Bloch-Floquet boundary conditions are applied at the lateral boundaries of the model to simulate a periodic plate with infinite lateral dimensions. The Bloch-Floquet wavenumber k_{B} corresponds to the incident wave. The solid part of the FE model is meshed by tetrahedral elements while the acoustic domains are discretized using the swept mesh method to generate prism elements as shown in Fig. 5. The sound transmission spectra in the 100 Hz to 2 kHz region are computed from

$$\mathrm{STL} = 10 \log \frac{P_{\mathrm{out}}}{P_{\mathrm{in}}} \text{ [dB]} \tag{3}$$

with P_{in} and P_{out} corresponding to the sound power evaluated at the structure-fluid interaction boundaries. Fig. 6 illustrates the resulting STL trend of the considered cell resonators, and Fig. 7 the dynamic responses of the sandwich structure for selected frequencies.

In Fig. 6, the bare panel without internal KC resonators is depicted with a dashed black line. A significant insulation loss of the bare panel is visible around 800 Hz which is associated with the resonance of both panels acting as a piston. To improve the insulation behavior in this frequency region, arrays made from the isometric KC and the 90° full-twisted structure are embedded and tuned by adjusting the ligament diameter. The isometric KC array displays a single peak in the STL in the targeted region where the KC structure exhibits mass-spring-like deformation as shown in Fig. 7 A. Yet, implementing this resonator reduces the insulation above 1 kHz compared to

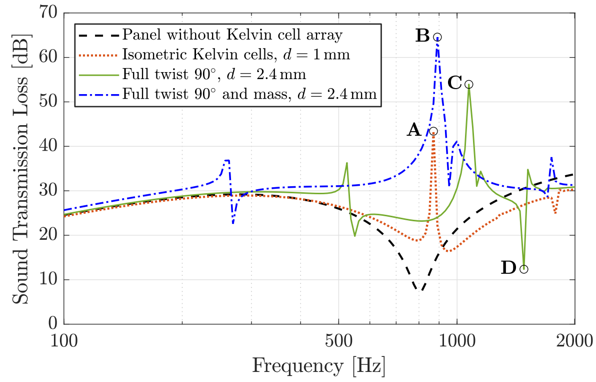

Figure 6: Sound Transmission Loss from 100 Hz to 2 kHz for different sandwich panel arrangements with KC resonators.

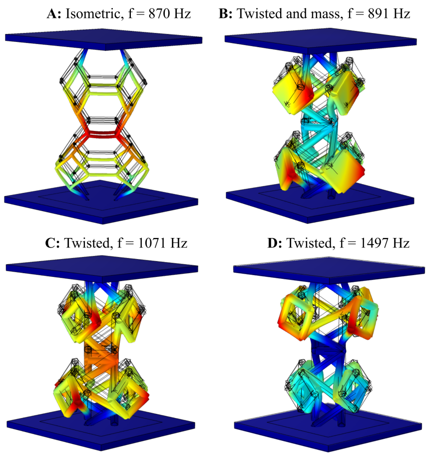

Figure 7: Dynamic deformation shapes of the KC resonators at selected frequencies (compare Fig. 6).

the bare panel. Applying the twisted KC array, however, introduces three peaks to the STL trend and overcomes the performance loss in the 800 Hz region. It is found that all STL peaks are governed by extension-rotation deformations at twisted face elements, shown in Fig. 7 C at 1071 Hz, for the sake of illustration. The improved trend obtained from twisted resonators is disrupted by two sharp dips near the peak values, *e. g.* noticeable at 1479 Hz. Here, the resonant characteristics of the array induce a strengthened coupling of the sandwich plate's out-of-plane displacements and, therefore, adversely affect the insulation performance. As a last illustration and test case, the twisted array is modified and non-central inertia is added by coating the empty spaces within all eight square faces with steel masses; each adding 7 % of the array weight to the system. The resulting STL spectrum indicates significant improvements within a wide band of nearly 500 Hz and a significant peak at 891 Hz (see Fig. 7 B). Compared to the twisted cell array without mass, the frequency of the first peak is lowered. Similarly, the resonant-induced dip observed at 1479 Hz is tuned down, not displaying a noticeable adverse impact on the insulation performance in the frequency range of consideration. Altogether, the discussed test cases demonstrate the applicability of KC resonators, with twisted cells introducing additional tunable resonances in the targeted frequency range and allowing for straightforward inertia amplification based on the KC lattice geometry.

Conclusions

The Kelvin cell geometry is proposed to serve as a fundamental unit for a locally resonant acoustic metamaterial for vibration insulation in the lower frequency range. By applying geometrical transformations on the cell ('twisting'), topologically equivalent designs to the reference structure are introduced with the possibility to tune their dynamic behaviour. In particular, an eigenfrequency analysis indicated that such twisting could provide a mechanism to target the cell dynamics and resonance characteristics, allowing to shift the eigenvalues and their relative spacing. At selected modes, twisting enforces coupling dynamics between extensional and torsional deformations. The effect may provide a leverage point for designing translational-rotational resonators with the lattice allowing for adjustable rotational inertia. Different cell arrangements are tested as meta-resonators embedded in a sandwich panel for sound transmission applications. Example results show that peak locations and amplitude values of the STL are tunable by twisting the cell and adjusting the lattice parameters. The tested KC structures show potential to enhance the STL performance at the cost of narrow-banded dips to adversely excited resonant modes. Exploiting the extensional-rotational coupled modes by embedding mass at the faces of twisted cells successfully prevents these dips and improves the STL performance. Further investigations seek to study the impact of twisting on the dispersion characteristics to potentially steer the bandgap generation to desired frequency ranges and possibly achieve a metamaterial with broadband performance in the lower-frequency regime.

References

[1] C. Claeys et al. 'A lightweight vibro-acoustic metamaterial demonstrator: Numerical and experimental investigation'. In: *Mechanical Systems and Signal Processing* 70-71.8 (2016).

[2] Luca D'Alessandro et al. '3D auxetic single material periodic structure with ultra-wide tunable bandgap'. In: *Scientific reports* 8.1 (2018).

[3] Emanuele Baravelli and Massimo Ruzzene. 'Internally resonating lattices for bandgap generation and low-frequency vibration control'. In: *Journal of Sound and Vibration* 332.25 (2013).

[4] Xiyue An et al. '3D acoustic metamaterial-based mechanical metalattice structures for low-frequency and broadband vibration attenuation'. In: *International Journal of Solids and Structures* 191-192.8 (2020).

[5] Marco Moscatelli et al. 'Band-gap structure in two- and three-dimensional cellular locally resonant materials'. In: *Journal of Sound and Vibration* 454.5485 (2019).

[6] Huina Mao et al. 'Twist, tilt and stretch: From isometric Kelvin cells to anisotropic cellular materials'. In: *Materials & Design* 193 (2020).

[7] Huina Mao, Romain Rumpler and Peter Göransson. 'An inverse method for characterisation of the static elastic Hooke's tensors of solid frame of anisotropic open-cell materials'. In: *International Journal of Engineering Science* 147.1–2 (2020).

[8] Huina Mao, Romain Rumpler and Peter Göransson. 'A note on the linear deformations close to the boundaries of a cellular material'. In: *Mechanics Research Communications* 111.6 (2021).

[9] Zibo Liu et al. 'Broadband locally resonant metamaterial sandwich plate for improved noise insulation in the coincidence region'. In: *Composite Structures* 200.6 (2018).